Developmental Cell
Article

# *Sox2* in the Dermal Papilla Niche Controls Hair Growth by Fine-Tuning BMP Signaling in Differentiating Hair Shaft Progenitors

Carlos Clavel,[1,2] Laura Grisanti,[1,2] Roland Zemla,[1,2] Amelie Rezza,[1,2] Rita Barros,[6] Rachel Sennett,[1,2] Amin Reza Mazloom,[4] Chi-Yeh Chung,[1,2] Xiaoqiang Cai,[2,3] Chen-Leng Cai,[2,3] Larysa Pevny,[7] Silvia Nicolis,[8] Avi Ma'ayan,[4] and Michael Rendl[1,2,5,*]

[1]Black Family Stem Cell Institute
[2]Department of Developmental and Regenerative Biology
[3]Center for Molecular Cardiology of the Child Health and Development Institute
[4]Department of Pharmacology and Systems Therapeutics
[5]Department of Dermatology
Mount Sinai School of Medicine, New York, NY 10029, USA
[6]IPATIMUP, University of Porto, 4200-465 Porto, Portugal
[7]Department of Genetics, University of North Carolina, Chapel Hill, NC 27599-7264, USA
[8]Department of Biotechnology and Biosciences, University of Milano-Bicocca, 20126 Milano, Italy
*Correspondence: michael.rendl@mssm.edu
http://dx.doi.org/10.1016/j.devcel.2012.10.013

## SUMMARY

**How dermal papilla (DP) niche cells regulate hair follicle progenitors to control hair growth remains unclear. Using *Tbx18*$^{Cre}$ to target embryonic DP precursors, we ablate the transcription factor *Sox2* early and efficiently, resulting in diminished hair shaft outgrowth. We find that DP niche expression of *Sox2* controls the migration speed of differentiating hair shaft progenitors. Transcriptional profiling of *Sox2* null DPs reveals increased *Bmp6* and decreased BMP inhibitor *Sostdc1*, a direct *Sox2* transcriptional target. Subsequently, we identify upregulated BMP signaling in knockout hair shaft progenitors and demonstrate that *Bmp6* inhibits cell migration, an effect that can be attenuated by *Sostdc1*. A shorter and *Sox2*-negative hair type lacks *Sostdc1* in the DP and shows reduced migration and increased BMP activity of hair shaft progenitors. Collectively, our data identify *Sox2* as a key regulator of hair growth that controls progenitor migration by fine-tuning BMP-mediated mesenchymal-epithelial crosstalk.**

## INTRODUCTION

Regulation of stem cell/progenitor functions is essential for tissue formation, growth, and maintenance throughout life. In regenerative tissues in particular, the rates of growth and replenishment through controlling stem cell/progenitor self-renewal and differentiation are critical for tissue homeostasis and adaptation to various environmental conditions, but the mechanisms underlying this important function are poorly understood. In regenerative tissues such as bone marrow, intestine, or hair follicles in the skin, signals from the microenvironment, called the stem cell niche, instruct stem and progenitor cells in their function (Moore and Lemischka, 2006; Walker et al., 2009).

In the hair follicle, a dynamic relationship between dermal papilla (DP) niche cells and epithelial stem cells/progenitors has been recognized for many years (Driskell et al., 2011; Hardy, 1992; Millar, 2002; Schneider et al., 2009; Sennett and Rendl, 2012; Yang and Cotsarelis, 2010). Mesenchymal-epithelial signals exchanged between dermal condensates (DP precursor cells) and stem cells in nascent hair placodes coordinate embryonic hair follicle formation (Hardy, 1992; Millar, 2002). Stem cells are set aside in the upper part of the down-growing follicle (Nowak et al., 2008), while matrix cell progenitors, direct stem cell progeny at the base of follicle bulbs, engulf DP precursor cells to form the DP of mature hair follicles (Millar, 2002; Schneider et al., 2009). During postnatal hair growth, DP cells then act as a signaling center to direct the surrounding matrix cells to proliferate, migrate upward, and differentiate into the multiple progenitor cell lineages of the outgrowing hair shaft and its guiding inner root sheath channel (Schneider et al., 2009; Sennett and Rendl, 2012). This morphogenetic sequence is repeated in three separate waves during mouse embryonic hair follicle development, giving rise to guard, awl/auchene, and zigzag hair follicle types (Figure 1A) (Schlake, 2007). First wave guard hairs are the longest hairs without kinks and bends, and are considered to have tactile function, much like whiskers. Second wave awl hairs are shorter than guard hairs, and auchene hairs look much like awl hairs, but with a unique identifying bend. Zigzag hairs typically have two kinks in the hair shaft. After active hair growth, follicles undergo cycles of destruction, rest, and regrowth to form a new hair follicle in a process of DP niche/stem cell communication that is reminiscent of embryonic follicle morphogenesis (Blanpain and Fuchs, 2009; Hsu and Fuchs, 2012; Sennett and Rendl, 2012).

During embryonic and adult follicle formation, the activation of signaling pathways such as WNT, tumor growth factor β (TGFβ), and fibroblast growth factor (FGF), and the inhibition of BMP signaling in follicle stem cells are essential (Hsu and Fuchs,

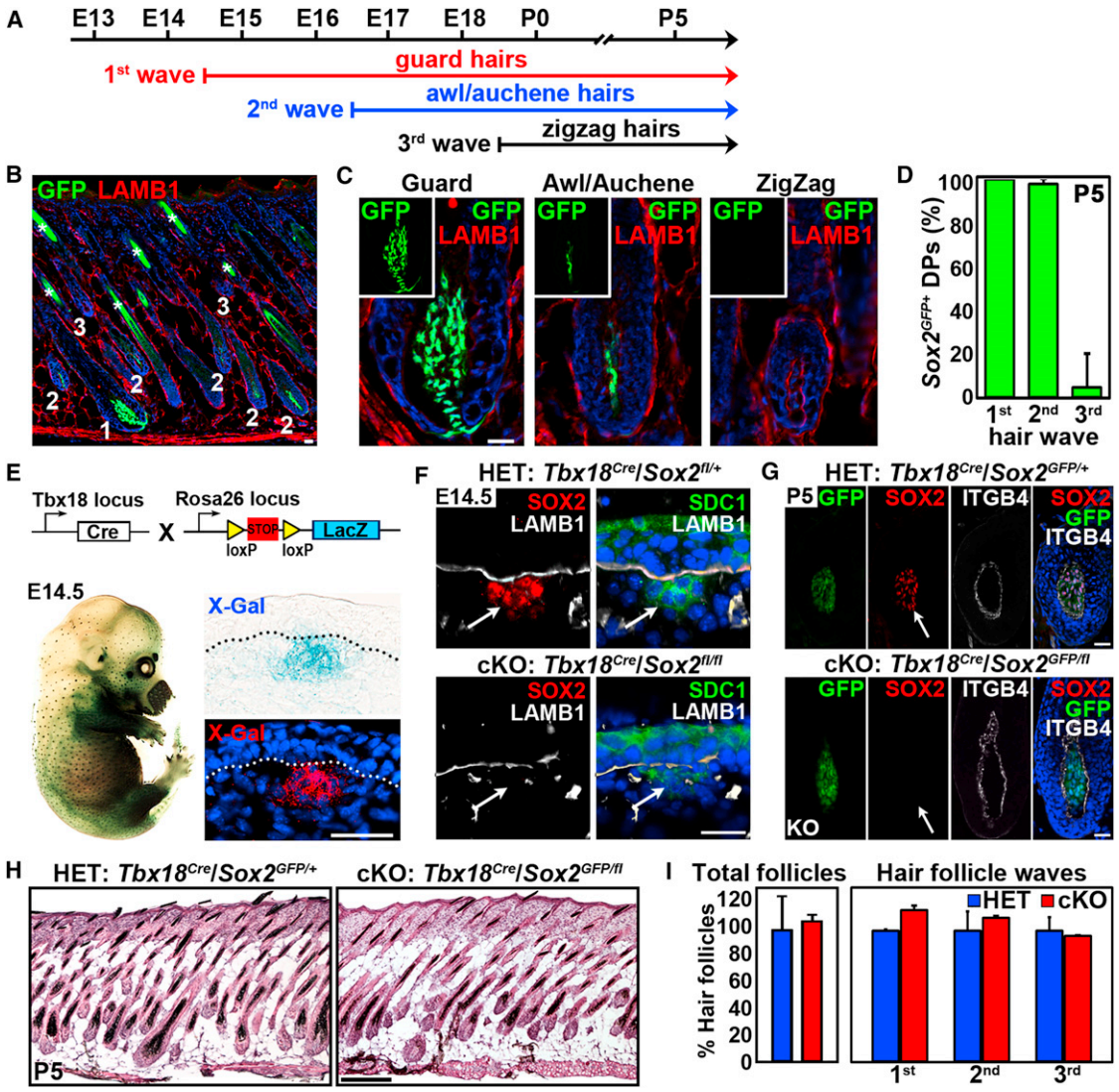


**Figure 1. *Sox2* Ablation in DP Precursors Does Not Affect Hair Follicle Formation**

(A) Schematic of the three major hair follicle formation waves during embryonic morphogenesis.

(B) *Sox2* expression analysis (green) in postnatal day P5 skin of $Sox2^{GFP}$ knockin reporter mice. LAMB1 stained the basement membrane (red). Nuclei are highlighted with DAPI (blue). Asterisk marks autofluorescence of hair shafts. Note GFP is expressed in DPs of first wave guard (1) and second wave awl/auchene (2) hair follicles. DPs of third wave zigzag follicles (3) do not express *Sox2*.

(C) High-magnification examples of hair follicle types with $Sox2^{GFP}$ positive and negative DPs.

(D) Quantification of $Sox2^{GFP}$ positive DPs in P5 follicles of all three waves. n = 130 hairs per mouse. Data are mean ± SD from 3 mice.

(E) Targeting of DP precursor cells with $Tbx18^{Cre}$. Top: Schematic of $Tbx18^{Cre}$ crossed with $R26R^{LacZ}$ reporter line. Bottom: Whole-mount X-Gal stained $Tbx18^{Cre}/R26R^{LacZ}$ embryo showed robust Cre activity in a hair follicle distribution at E14.5. Histological analyses of sectioned embryo with Cre reporter activity in DP precursors.

(F) Efficient ablation of SOX2 protein in $Tbx18^{Cre}/Sox2^{fl/fl}$ conditional knockout (cKO) embryo. SOX2 immunofluorescence was absent in cKO dermal condensates (arrows) at E14.5. Syndecan-1 (SDC1) labeled dermal condensates and LAMB1 marked the basement membrane.

(G) Immunofluorescence staining for SOX2 at P5. SOX2 is absent in null DPs (arrow) in a $Sox2^{GFP}$ reporter background.

(H) Hematoxylin/eosin staining of *Sox2* heterozygous (HET; $Tbx18^{Cre}/Sox2^{GFP/+}$) and conditional knockout (cKO; $Tbx18^{Cre}/Sox2^{GFP/fl}$) skins at P5.

(I) Quantification of total hair follicles and of follicles from the three waves at P5. n = 75 hairs per mouse. Data are mean ± SD from 2 mice.

Scale bars, 25 μm (A–G) and 250 μm (H). See also Figures S1 and S2.

2012; Sennett and Rendl, 2012; Lee and Tumbar, 2012). Similarly, during active hair growth, WNT, FGF, Notch, and BMP signaling in matrix progenitor cells is important for successful differentiation into the outgrowing hair shaft (Andl et al., 2004; DasGupta and Fuchs, 1999; Kobielak et al., 2003; Kulessa et al., 2000; Lee et al., 2007). While the essential roles of these signaling pathways have been extensively studied in epithelial stem cells/progenitors, direct genetic testing of DP niche signals has been lacking until very recently (Enshell-Seijffers et al., 2010) due to the long-standing absence of gene ablation tools for the

DP. Similarly, the underlying transcriptional control of DP niche signals and of the specialized niche cell fate that distinguishes the DP from regular dermal fibroblasts is currently largely unknown.

The transcription factor *Sox2* is a crucial cell fate determinant in stem cells/progenitors in multiple developmental contexts. It regulates cell fate decisions in retinal progenitor cells (Taranova et al., 2006) and neural (Pevny and Nicolis, 2010) and embryonic stem cells (Boyer et al., 2005), and it is a key factor in pluripotency reprogramming (Takahashi and Yamanaka, 2006). Recently, *Sox2* was shown to play a role in maintaining adult stem cells in several organ systems (Arnold et al., 2011). In skin, *Sox2* is not expressed in hair follicle stem cells, but is one of the highest expressed transcription factors in the DP, first identified in a screen of DP signature genes in growing hair follicles (Rendl et al., 2005). Subsequently, *Sox2* expression was confirmed in embryonic DP precursors and postnatal DPs of growing follicles (Biernaskie et al., 2009; Driskell et al., 2009; Tsai et al., 2010), and considered absent during the hair cycle (Biernaskie et al., 2009). The physiological function of Sox2 during follicle formation and growth is currently unknown.

In this study, we directly test the role of *Sox2* in controlling DP function during follicle formation and growth by ablating *Sox2* in the DP during embryonic hair follicle formation. We utilize $Tbx18^{Cre}$ as a genetic driver that targets embryonic DP precursor cells at the earliest stage of hair follicle formation (Grisanti et al., 2012). In the absence of *Sox2*, we find a strong reduction of postnatal hair outgrowth of the three *Sox2*-positive hair follicle types and identify slowed migration of differentiating hair shaft progenitors. We then link reduced migration and slowed hair shaft production to altered expression of DP-derived BMP regulators *Bmp6* and *Sostdc1* and to precocious, increased BMP signaling activity in hair shaft progenitors. Fittingly, a fourth *Sox2*-negative hair follicle type naturally displays slower growth, reduced migration, and increased BMP activity in hair shaft progenitors. These data reveal an essential role of *Sox2* in the transcriptional control of the mesenchymal niche to orchestrate hair growth in its interaction with epithelial progenitors.

## RESULTS

### *Sox2* Ablation in Embryonic DP Precursors Does Not Affect Hair Follicle Formation

To determine *Sox2* expression throughout hair follicle development, we first carefully mapped the *Sox2* expression pattern with $Sox2^{GFP}$ knockin reporter mice that express GFP under the control of the endogenous *Sox2* promoter (Ferri et al., 2004). At embryonic day E14.5, GFP was strongly expressed in DP precursor cells of developing guard hair follicles during the first wave of hair follicle induction (arrow in Figure S1A available online). At E16.5, DP precursors of second wave follicles of the awl/auchene hair type also expressed GFP (arrowhead). DP precursor cells of third wave zigzag follicles at E18.5, however, did not express *Sox2* (asterisk), confirming a previous report where zigzag DPs lacked *Sox2* expression at E18.5 with a *Sox2* transgenic reporter (Driskell et al., 2009). Quantification of $GFP^+$ DPs confirmed labeling of nearly 100% first and second wave DPs, while all third wave zigzag DPs lacked *Sox2* expression activity (Figures S1B and S1C).

This hair type-specific distribution of *Sox2* continued during postnatal hair growth (Figures 1B–D). At P5, first wave guard hairs are the longest follicles and were identified by distinctly large DP compartments, while third wave zigzag follicles were clearly recognized as the shortest hair follicle population with small DPs (Figures 1B and 1C). Second wave awl/auchene follicles are the second-longest follicles with thin, long DPs (Figures 1B and 1C). Similar to embryonic stages, all DPs of first wave guard and second wave awl/auchene hair follicles were $GFP^+$, while zigzag DPs remained negative (Figure 1D) (Driskell et al., 2009). During the subsequent destruction (catagen) and resting (telogen) phase of the hair cycle, GFP continued to be expressed in DPs (Figure S1D) that were identified as *Lef1-RFP* cell clusters (Greco et al., 2009; Rendl et al., 2005), although *Sox2* was previously reported absent in the DP during the hair cycle (Biernaskie et al., 2009). To confirm *Sox2* expression in adult DPs, we identified SOX2 protein in $RFP^+$ DPs by immunofluorescence staining using a SOX2-specific antibody (Figure S1E). Taken together, these data demonstrate *Sox2* expression in DP precursors and mature DPs in most hair types during morphogenesis and the hair cycle.

To determine whether *Sox2* in the DP niche plays an important role in hair follicle formation and growth, we next sought to ablate *Sox2* in DP cells as early as possible during development. In an effort to establish gene targeting of DP precursor cells, we recently identified in a screen of candidate DP reporters *Tbx18* knockin lines (Figures 1E and S1F-S1I) with robust expression in these cells (Grisanti et al., 2012). X-gal staining in whole-mount $Tbx18^{LacZ}$ embryos showed *Tbx18* expression in skin in a hair follicle pattern (Figure S1G) and in sections in dermal condensates of DP precursor cells (Figure S1H). No expression was found in skin prior to E14.5 (data not shown). In other body areas outside of skin, *Tbx18* expression was detected in somites, limbs, whiskers, meninges, and epicardium (Figure S1I), as previously described (Cai et al., 2008; Kraus et al., 2001). Next, in crosses of $Tbx18^{Cre}$ (Cai et al., 2008) with $R26R^{LacZ}$ reporter mice (Soriano, 1999), we detected Cre activity in developing hair follicles at E14.5 (Figure 1E, left). Histological analyses of embryo sections revealed Cre reporter activity in DP precursor cells already at E14.5 during first wave follicle induction (Figure 1E, right), suggesting that $Tbx18^{Cre}$ could be used efficiently to ablate *Sox2* in floxed mice. $Tbx18^{Cre}$ is also active in second and third wave DP precursors at E16.5 and E18.5 (data not shown). At E16.5 and later developmental stages, *Tbx18* expression and Cre activity also become more widespread throughout the dermis (data not shown). A detailed characterization of *Tbx18* reporter and Cre activities at all developmental stages was reported recently (Grisanti et al., 2012).

To conditionally knock out *Sox2* in DP precursor cells we next crossed $Tbx18^{Cre}$ with $Sox2^{fl/fl}$ lines, in which the *Sox2* coding sequence is flanked by LoxP sites for Cre-mediated recombination and gene ablation (Favaro et al., 2009). In addition, we generated a *Sox2* conditional knockout variation, in which one *Sox2* floxed allele was replaced by the $Sox2^{GFP}$ knockin allele, which allowed for detection of *Sox2* promoter activity even after *Sox2* ablation. SOX2 immunofluorescence staining demonstrated efficient SOX2 ablation in dermal condensates of first and second wave hair follicles at E14.5 and E16.5 (Figures 1F and S2A). Costaining for dermal condensate marker SDC1

(Syndecan-1) (Richardson et al., 2009) confirmed positive identification of DP precursor cells in the cKO, suggesting that dermal condensates formed despite efficient *Sox2* ablation. Alkaline phosphatase staining at E18.5 identified DPs in hair follicles from all three waves (Figure S2B) and hematoxylin/eosin staining at P0 showed follicles with normal size and distribution in cKO skins (Figure S2C). Quantification of total hair follicles (Figure S2D) and hair follicle types per wave (Figure S2E) confirmed normal formation in embryonic skins with *Sox2* cKO DPs. Similarly, follicle maturation after birth progressed normally without *Sox2*. Immunofluorescence staining confirmed absence of SOX2 protein in postnatal cKO guard hair follicles, which continued to express GFP from the $Sox2^{GFP}$ reporter allele (Figure 1G). Follicles from all three waves developed without obvious morphological differences between HET and cKO skins at P5 (Figure 1H). Quantification of hair follicles and of follicle types per wave was virtually identical in HET and cKO (Figure 1I). Progression through the adult hair cycle was unaffected as well. All hair cycle stages, as determined by established morphological criteria (Müller-Röver et al., 2001), were observed with similar timing and unaltered follicle morphologies in cKO skins (Figure S2F). Total hair follicle counts were unchanged (Figure S2G) and quantification of follicles in catagen, telogen and anagen stages did not show any changes in cKO skins (Figure S2H). From these data we conclude that although *Sox2* is efficiently ablated in early dermal condensates, its absence does not affect initial follicle formation and hair cycle progression, suggesting that this transcription factor is not required for these processes.

## *Sox2* Ablation in the DP Impairs Hair Shaft Outgrowth after Birth

While follicle morphogenesis and cycling was not affected by ablation of *Sox2* in the DP, we noticed markedly delayed hair shaft outgrowth. External hair shafts of first wave guard hair follicles normally break through the epidermis and become externally visible around postnatal day P4–P5. By P8, guard hair shafts of heterozygous (HET) control pups had grown out substantially to start forming the hair coat, but in cKO skins they were strongly growth diminished (Figure 2A, magnification of insert in Figure 2B). Precise measurement and quantification of guard hair shaft lengths at P8 and later stages showed a significant reduction at all time points (Figure 2C). Importantly, the difference in hair shaft lengths increased over time, but the relative length of shortened hairs in cKOs compared to HETs remained constant at 65%–70% (Figure 2D). This indicates that the diminished hair outgrowth in *Sox2* cKO guard hair follicles proceeds at a constantly reduced speed. It further suggests that it is not the result of a developmentally delayed hair growth start that would then progress at a normal speed.

Next we tested whether *Sox2* expressing second wave awl/auchene hair shafts were also shorter in cKO pups, and whether third wave zigzags that do not express *Sox2* were unaffected, as predicted based on the differential *Sox2* expression in the DP compartments of these hair types. For this, we shaved off hair shafts at P20, classified the hair types based on established length, shape, and medulla size criteria (Schlake, 2007) and measured their lengths. As shown in Figure 2E, guard and awl/auchene hairs were considerably shorter in *Sox2* cKO, but zigzag lengths were comparable to HET control. Quantification of shaft lengths confirmed a significant reduction of 20%–55% (Figure 2F).

To understand the mechanistic underpinnings of the hair shaft outgrowth reduction, we next determined whether proliferation of matrix progenitor cells is affected by *Sox2* ablation in the mesenchymal DP compartment. Immunofluorescence stainings for Ki67, which marks all proliferating cells, did not show any significant differences between HET and cKO follicles (Figure 2G). In both, 100% of matrix progenitor cells were Ki67 positive below the Auber's line (Figure 2G), which divides the matrix into a proximal and distal half at the mid-DP level (Vanscott et al., 1963). Similarly, staining for phospho-Histone H3 (PH3) to identify cells in mitosis, a short and infrequently detected event during the cell cycle, was also comparable in HET and cKO hair bulbs (Figure 2H). To determine whether increased cell death could possibly cause a loss of matrix cells, we stained for active caspase-3 that labeled cells undergoing apoptosis. No significant cell death was detected in cKO follicles and HET controls (Figure S3A). These data suggest that ablation of *Sox2* in DPs does not alter the proliferation rate or cause increased cell death of surrounding matrix cells at the follicle base.

Next we determined whether aberrant differentiation into the cell lineages of the hair shaft and inner root sheath (IRS) could contribute to reduced hair growth in *Sox2* ablated follicles. Immunofluorescence stainings for biochemical markers in P5 HET and cKO guard hair follicles revealed normal Keratin-14 (K14) expression in outer root sheath and matrix progenitor cells (Figure 2I). Hair shaft cortex and medulla differentiation markers AE13 and AE15, which label hair keratins and keratohyalin, respectively, were also unchanged (Figures 2J and 2K). AE15 was further detected in the IRS as expected. Additional nuclear staining of GATA3 in the companion layer of the IRS was present in a normal pattern as well (Figure 2L). Similar unchanged staining for differentiation marker AE13 was already detectable at P0 (Figure S3B). Finally, to evaluate whether *Sox2* ablation impacts normal DP maturation in developed follicles we analyzed expression of known DP markers AP, HHIP, and WIF1 (Rendl et al., 2005), all of which appeared to be present (Figure S3C). Taken together, these data indicate that *Sox2* in the DP is critical for the normal speed of hair shaft outgrowth in guard, awl, and auchene follicles by a mechanism other than perturbed proliferation or differentiation of matrix progenitor cells.

## *Sox2* Ablation in DP Leads to Delayed Progenitor Migration into the Differentiating Hair Shaft Compartment

Since neither matrix cell proliferation nor hair shaft differentiation was affected in cKO hair follicles, we next analyzed whether altered cell migration from the matrix compartment into the differentiating hair shaft could possibly explain the delay of hair shaft production. To label matrix cells and determine their rate of transition into the hair shaft area, we performed bromodeoxyuridine (BrdU) pulse-chase experiments. A single BrdU injection was administered (pulse), and labeled cells were analyzed between 2 and 54 hr later in harvested skin tissues (chase) (Figure 3A). In this assay, highly proliferative matrix cells at the follicle base incorporate BrdU label during the S-phase of the cell cycle (Figure 3B, left) and are traced as they migrate into the hair shaft

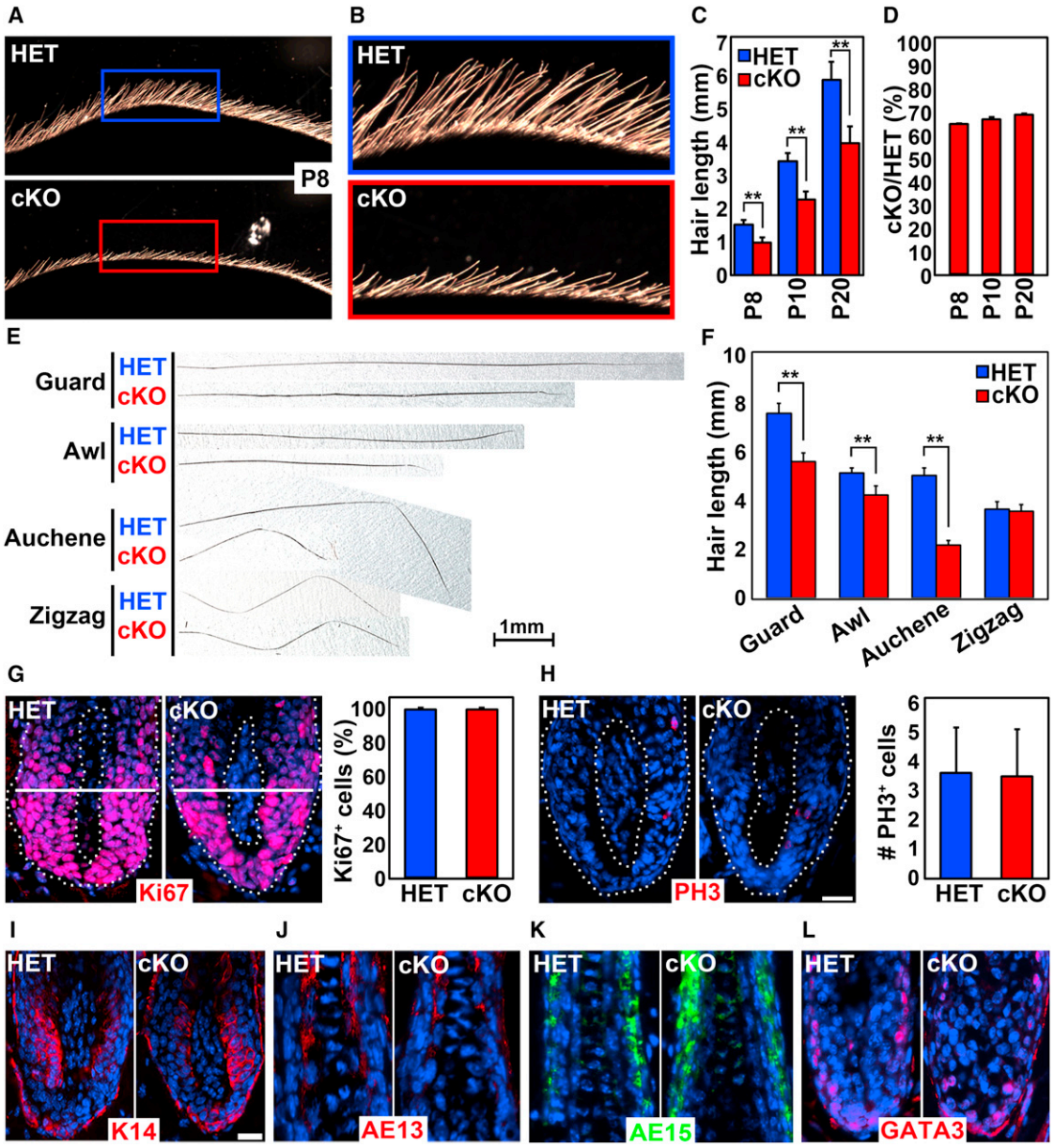


**Figure 2. *Sox2* Ablation in the DP Strongly Impairs Hair Shaft Outgrowth**

(A) Side view of dorsal skin with outgrowing hair shafts at P8. Hair shafts are shorter in *Sox2* cKO skin.

(B) High-magnification view of HET (blue frame) and cKO (red frame) inserts. First wave guard hair shafts are of considerable length by P8 in HET, but are much shorter in cKO.

(C) Quantification of guard hair shaft lengths. n = 20 guard hairs per mouse. Data are mean ± SD from three mice. $^{**}p < 0.01$.

(D) Relative guard hair shaft length reduction remains constant at all time points.

(E) Examples of HET and cKO hair shafts from all four hair types at P20. Note that *Sox2* expressing guard, awl, and auchene hairs were shorter in cKO. *Sox2*-negative zigzag hairs were unchanged.

(F) Quantification of hair shaft lengths of P20 clipped hairs. n = 20 hairs per hair type. Data are mean ± SD from two mice. $^{**}p < 0.01$.

(G) Immunofluorescence staining of proliferation marker Ki67. Dotted line marks basement membrane. Right: Quantification of $Ki67^+$ cells below Auber's line (white). n = 10 guard hairs per mouse. Data are mean ± SD from two mice.

(H) Immunofluorescence staining of mitosis marker phospho-histone H3 (PH3). Right: Quantification of $PH3^+$ cells in guard hair bulbs. n = 20 guard hairs per mouse. Data are mean ± SD from 2 mice.

(I–L) Immunofluorescence staining of (I) matrix marker K14 and hair shaft differentiation markers (J) AE13 (hair cortex), (K) AE15 (IRS), and (L) GATA3 (inner root sheath).

Scale bar is 25 μm. See also Figure S3.

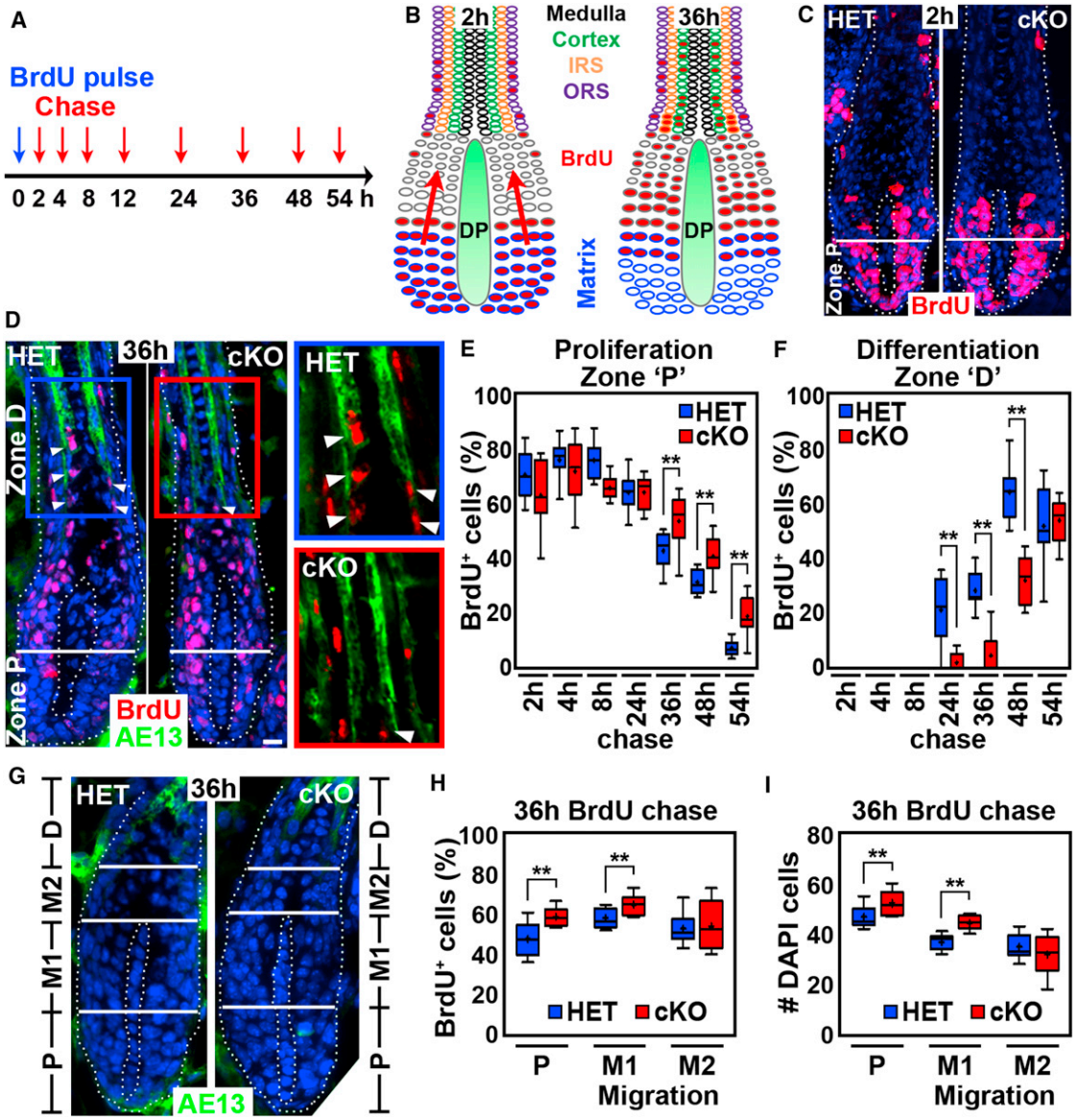


**Figure 3. Sox2 Ablation Impairs Progenitor Migration during Hair Growth**

(A) Pulse/chase BrdU labeling to track proliferating and migrating matrix cells. Timeline of BrdU injection at P5 (pulse) and chase time points for tissue harvest and BrdU label analysis (red arrows).

(B) Schematic of initial BrdU uptake (2 hr) and of migration of matrix cells toward the hair shaft differentiation areas (36 hr).

(C) BrdU immunofluorescence staining at 2 hr. Proliferation zone "P" is below Auber's line (white). Note robust BrdU uptake in both *Sox2* HET and cKO follicles.

(D) BrdU/AE13 double immunofluorescence staining at 36 hr. Differentiation zone "D": BrdU$^+$ cells in the differentiating hair cortex labeled by AE13 (arrowheads). Note decreased BrdU$^+$ matrix cells migrating into zone "D" in cKO. Right: Inserts show higher magnification views of zone "D" in HET (blue frame) and cKO (red frame). Dotted line marks basement membrane. Nuclei are counterstained with DAPI. Scale bars are 25 μm.

(E and F) Quantification of BrdU$^+$ cells in zones "P" and "D." Note delayed exit of zone "P" and entry into zone "D" of BrdU$^+$ matrix cells in follicles with *Sox2* null DPs.

(G) Migration zone "M" between proliferation zone "P" and differentiation zone "D." Zone "M" is subdivided into proximal zone "M1" and distal zone "M2" at the level of the distal DP tip. AE13 staining defines the border to differentiation zone "D."

(H and I) Quantification of BrdU$^+$ cells and total cell numbers (as DAPI$^+$ nuclei) in zones "P," "M1," and "M2" at 36 hr. Note increased BrdU$^+$ cells (H) and total cell numbers (I) in zones "P" and "M1" in follicles with *Sox2* null DPs.

All box-and-whisker plots: mid-line, median; mean, plus symbol; box, 25$^{th}$ and 75$^{th}$ percentiles; whiskers, 10$^{th}$ and 90$^{th}$ percentiles. N = 10 guard hairs/time point. Counts are from three (E and F) and two (H and I) independent experiments. $^{**}p < 0.01$; $^{*}p < 0.05$.

area (Figure 3B, right). Already 2 hr after BrdU injection the majority of matrix cells of *Sox2* HET follicles were labeled in the proliferating Zone "P" below the Auber's line (Figure 3C). Importantly, equally rapid labeling occurred in cKO follicles, again demonstrating comparable matrix cell proliferation. In both HET and cKO matrix compartments, BrdU labeling peaked

at 4 hr after injection (Figure 3E). After 24 hr, the number of labeled matrix cells started to decrease in both HET and cKO follicles, as the cells began to move upward toward the hair shaft (Figure 3E). By 36 hr, depletion of $BrdU^+$ cells in Zone "P" occurred more rapidly in HET follicles (Figures 3D and 3E), suggesting that matrix cell exit from this area is significantly delayed in cKO follicles (Figure 3E). Conversely, at 36 hr, multiple $BrdU^+$ cells in HET follicles had already entered the differentiation zone "D," identified as the AE13 labeled cortex of the hair shaft (Figure 3D, magnification of insert on the right; and Figure 3F). Only sporadic BrdU/AE13 double-positive cells were found in cKO follicles. This significant migration delay in cKO follicles remained detectable up to 48 hr (Figure 3F).

We next had a closer look at the intermediary zone that connects the proliferating and differentiating zones "P" and "D" (Figure 3G). This migration Zone "M" consists of matrix cells that transition from the proliferating to the differentiating areas. Analysis of cKO guard hair follicles revealed increased numbers of $BrdU^+$ cells in the proximal half between the Auber's line and the level of the distal DP tip (Zone "M1")(Figure 3H), but unchanged BrdU labeled cell numbers in the distal Zone "M2," compared to control HET follicles. This suggests a backlog of migrating cells that reaches up to the distal end of the DP. Indeed, careful analysis of total cell numbers revealed increased cellularity in zones "P" and "M1," but not in "M2" (Figure 3I). The accumulated cells do not appear to reach a level that would distort the follicle architecture. Analysis of apoptosis by staining for activated caspase-3 did not show increased cell death (Figure S3A).

From these data we conclude that the upward movement of matrix progenitor cells is significantly impaired as they differentiate into the hair shaft cell lineages. This suggests that slowed hair shaft outgrowth in follicles with *Sox2* ablated DPs is caused by the delayed migration of differentiating matrix cells into the hair shaft compartment.

## *Sox2* Ablation Alters DP Signature Gene Expression

To gain insights into how ablation of the transcription factor *Sox2* in the mesenchymal DP compartment may affect cell migration and hair growth in the epithelial compartment, we isolated *Sox2* knockout DP cells and determined genome-wide the potential gene expression changes. For this, hair follicles from $Tbx18^{Cre}/Sox2^{GFP}$ heterozygous and $Tbx18^{Cre}/Sox2^{GFP/fl}$ conditional knockout P5 skins were freshly isolated and single cells were stained for integrin-alpha 9 (ITGA9), a marker expressed by DP cells (Figure 4A) (Rendl et al., 2005; Tsai et al., 2010). Pure DP cells were then isolated by fluorescence-activated cell sorting (FACS) as $GFP^+/ITGA9^+$ cells, which prevented contamination with GFP-only touch dome cells and ITGA9-only dermal cells (Figure 4B; and data not shown). To verify high enrichment of DP cells, we also isolated negative cells as control population and compared by real-time PCR the expression of several known DP signature genes (Figure 4C). As expected, signature gene expression was > 30-fold enriched in $GFP^+/ITGA9^+$ cells.

We then proceeded with transcriptional profiling of two independently sorted biological replicates using Affymetrix GeneChip Mouse Gene 1.0 ST microarrays. Comparative analysis between HET and cKO samples and hierarchical clustering revealed significant >1.25-fold down- and upregulation of 840 and 223 genes, respectively (Figure 4D). We next grouped downregulated and upregulated gene lists into functional categories based on gene ontology classifications and determined the overall enrichment of categories compared to their representation in the genome. Significantly enriched functional categories of downregulated genes included protein transport, cell migration, WNT signaling, mesenchymal cell development, and extracellular matrix (Figure 4E, top). Significantly enriched categories of upregulated genes included transcriptional regulation, cytoskeleton, repressor, and growth (Figure 4E, bottom).

Real-time PCR further validated expression of several downregulated and upregulated genes in *Sox2* cKO DP cells (Figure 4F). Absence of any detectable *Sox2* mRNA levels confirmed 100% gene ablation efficiency. Several regulated genes were associated with signaling pathways that have been previously implicated in hair follicle formation and growth, such as *Notch1* and *Hey1* (Notch signaling), *Pbx1*, *Prdm1/Blimp1*, and *Sox18* (Figure 4F). Interestingly, among the most strongly regulated genes were WNT and BMP pathway regulators. Both signaling pathways are activated and essential during hair shaft differentiation (Andl et al., 2004; DasGupta and Fuchs, 1999; Kobielak et al., 2003; Kulessa et al., 2000), and recent evidence suggests a role in DP cells for follicle formation as well (Kishimoto et al., 2000; Rendl et al., 2008). In *Sox2* null DPs, the WNT inhibitors *Sfrp2* and *Wif1* were downregulated and upregulated, respectively (Figures 4E and 4F). *Sostdc1*, an inhibitor of both BMP and WNT signaling, was also strongly downregulated, while at the same time *Bmp6* was upregulated (Figures 4E and 4F). From this we conclude that in the absence of *Sox2*, the level of WNT signaling could be increased if the differential regulations of the inhibitors do not cancel each other out. We further conclude that BMP signaling should be tilted toward increased activation within the DP and hair epithelium, as both a BMP inhibitor is decreased and a BMP ligand is increased.

## Expression of BMP/WNT Inhibitor *Sostdc1* in DP Cells Is Directly Regulated by *Sox2*

Because the transition of proliferating matrix cells to the differentiating compartment is delayed in follicles with *Sox2* null DPs and BMP signaling has been previously reported to inhibit keratinocyte migration during wound healing (Kaiser et al., 1998), we focused our attention on the decreased expression of BMP/WNT inhibitor *Sostdc1* in *Sox2* ablated DP cells. First, we validated the microarray and real-time PCR regulation by direct analysis of *Sostdc1* expression in HET and cKO skin tissue by in situ hybridization. In HET hair follicles, *Sostdc1* was exclusively expressed in DP cells confirming the DP-specific expression of this previously identified signature gene (Rendl et al., 2005). In contrast, *Sostdc1* mRNA message was barely detectable in *Sox2* cKO DPs (Figure 5A). To test whether *Sox2* could regulate *Sostdc1* levels, we freshly isolated DP cells by FACS and lentivirally overexpressed *Sox2* (Figure 5B, left). As shown in Figure 5B (right), *Sox2* dramatically upregulated *Sostdc1* expression levels in DP cells, suggesting that this gene is controlled by *Sox2*.

Next we determined whether *Sox2* regulates *Sostdc1* as an immediate target gene by directly binding to regulatory regions in the *Sostdc1* promoter/enhancers. For this, we first identified potential target binding sites within ± 20kb of the *Sostdc1*

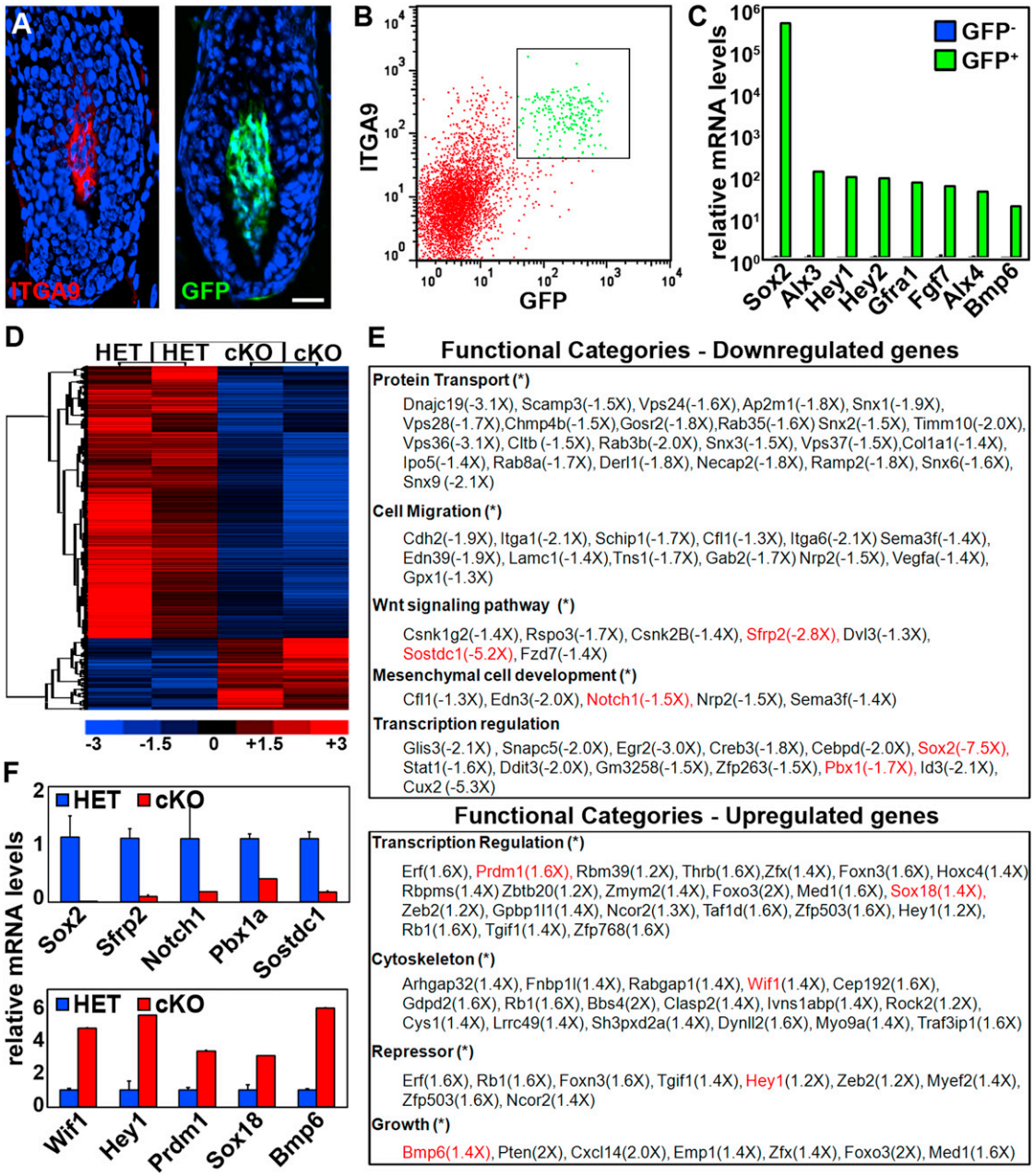


**Figure 4. *Sox2* Ablation in the DP Alters Its Gene Expression Signature**

(A–C) FACS sorting strategy to isolate *Sox2*$^{GFP}$/Integrin-alpha 9 double-positive DP cells from *Sox2* HET and cKO P5 skin for transcriptional profiling. (A) *Sox2*$^{GFP}$ and Itga9$^{+}$ DPs. Nuclei are counterstained with DAPI. Scale bar is 25 μm. (B) DP population is FACS isolated as *Sox2*$^{GFP+}$/ITGA9$^{+}$ cells. (C) Real-time PCR of sorted *Sox2*$^{GFP}$-positive and -negative cells.

(D) Heat map and clustering analysis of altered gene expression in microarrays from HET and cKO sorted P5 DPs.

(E) Functional gene ontology categories enriched in downregulated (top) and upregulated (bottom) genes in cKO DPs. Genes highlighted in red were corroborated by real-time PCR.

(F) Real-time PCR verification of downregulated and upregulated genes in cKO DPs. Data are mean ± SD (n = 2).

transcription start site by computing motif Fit-Conservation (FC) scores that address both sequence homology of a previously reported *Sox2* consensus binding motif (Figure 5C) (Fang et al., 2011) and sequence conservation of the motif within multiple mammalian species (Figure 5D). This analysis revealed two major candidate binding sites, at 1.5 kb downstream and 8 kb upstream of the transcription start site, respectively (Figure 5E, "S1," "S2").

We then sorted pure DP cells from hair follicles in vivo and immunoprecipitated *Sox2* after crosslinking protein bound to DNA. RT-PCR with primers amplifying the potential binding sites and also an unrelated control region ("N1") revealed no

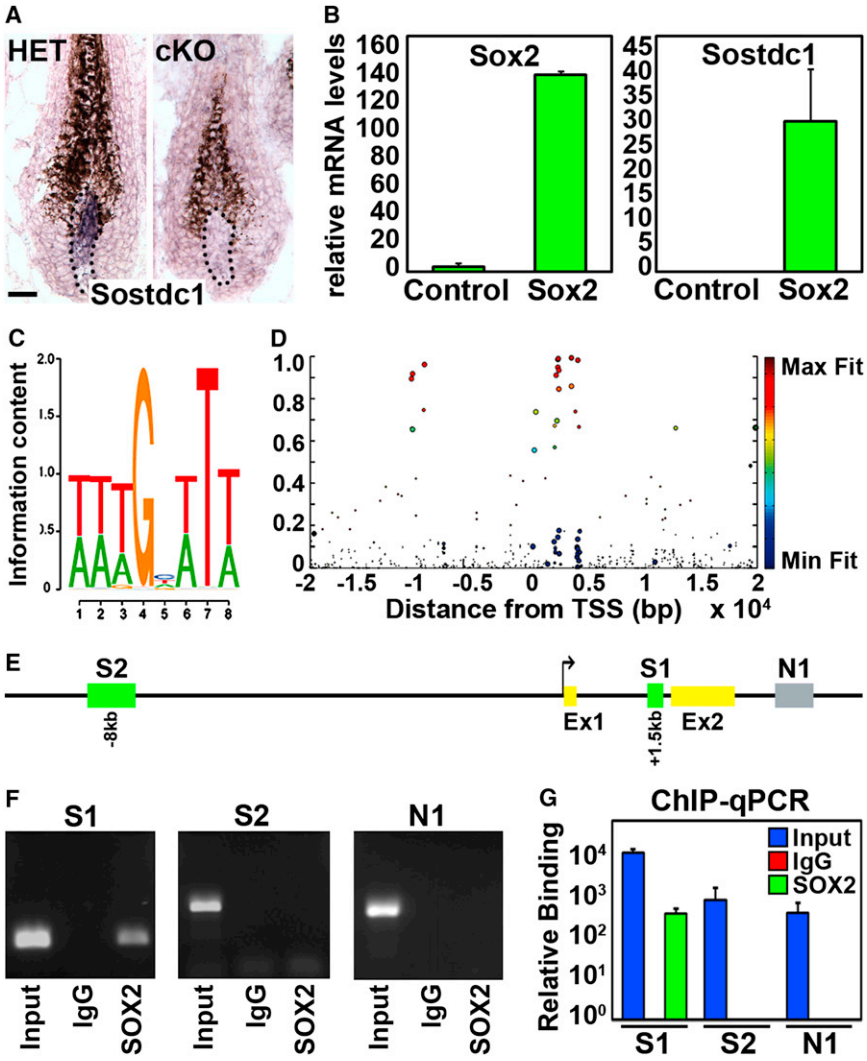


**Figure 5. Expression of BMP/WNT Inhibitor *Sostdc1* in DP Cells Is Directly Regulated by *Sox2***

(A) In situ hybridization for *Sostdc1* mRNA expression in *Sox2* HET and cKO guard hair follicle. Dotted line marks the basement membrane. Scale bar is 25 μm.

(B) Real-time PCR for *Sox2* (left) and *Sostdc1* (right) in isolated DP cells that lentivirally overexpress *Sox2*. Data are mean ± SD (n = 2).

(C) Predicted SOX2 binding site consensus sequence.

(D) Heat map of putative SOX2 binding sites in the *Sostdc1* genomic region based on consensus sequence and species conservation.

(E) Schematic of genomic region displaying two putative SOX2 binding sites, "S1" and "S2." "N1" is used as a control site.

(F) ChIP-PCR to detect SOX2 binding to conserved SOX2 binding sites "S1," "S2." "N1" is a control intronic fragment with no predicted site. Shown is one of two representative experiments.

(G) ChIP-qPCR analyses to assess relative binding of SOX2 to "S1," "S2" sites. Fold enrichments of immunoprecipitated DNA fragments are compared to control "N1" and presented relative to IgG. Data are mean ± SD of two independent experiments.

bound *Sox2* at the S2 and the negative control sites. However, specific binding of *Sox2* was identified at the S1 site within the first intron of the *Sostdc1* gene (Figure 5F). Quantitative real-time PCR of *Sox2* binding relative to IgG control showed a 400× enrichment at the S1 site (Figure 5G). Taken together, these chromatin immunoprecipitation and *Sostdc1* regulation experiments in freshly isolated DP cells suggest that *Sostdc1* expression is directly regulated by Sox2 and is therefore strongly decreased in cKO DP cells due to absence of *Sox2*.

## Precocious and Increased BMP Signaling Activity in Differentiating Hair Shaft Progenitors in Follicles with *Sox2* Ablated DPs

We next wondered whether the differential regulation of WNT inhibitors *Sfrp2* and *Wif1*, and the downregulation of the BMP/WNT inhibitor *Sostdc1* and upregulation of *Bmp6* would lead to increased WNT and BMP signaling within the epithelial compartment that could cause slowed hair shaft outgrowth. To determine the level of WNT signaling, we detected by immunofluorescence the nuclear staining of the WNT responsive transcription factor β-catenin, which in the absence of WNT signaling is only detectable at adherens junctions at the cell membrane. In both Sox2 HET and cKO follicles, nuclear β-catenin was present in differentiating hair shaft cells at normal levels (Figure S4A, arrows) (Merrill et al., 2001), suggesting that WNT signaling does not directly contribute to altered migration of differentiating hair shaft lineages. It was also detectable in the DP, but with slightly increased intensity in the cKO (Figure S4A, open arrowheads).

To detect cells with active BMP signaling, we stained for SMAD1,5, which becomes phosphorylated downstream of BMP receptor activation and translocates to the nucleus, where target genes are transcribed (Massagué et al., 2005). During early postnatal hair growth, active nuclear pSMAD1,5 can be detected in IRS cells, before expanding into differentiating hair shaft cortex and medulla at more mature stages (Andl et al., 2004; Kobielak et al., 2003). As judged by immunofluorescence staining for pSMAD1,5, BMP signaling was active in HET control follicles at P5 mostly in IRS cells, located outside the AE13-positive hair cortex (Figures 6A and S4B, arrowheads). By contrast, widespread pSMAD1,5 levels were already detectable in hair cortex and medulla cells within and inside the AE13 expression domain of cKO guard hair follicles (Figures 6A and S4B, open arrowheads). Quantification revealed ~75% pSMAD1,5-positive cells in the AE13 domain of cKO, while only ~15% were pSMAD1,5/AE13 double-positive in HET follicles (Figure 6B). In addition, widespread precocious BMP signaling activity was already visible in the IRS at P0 in ~90% of cKO guard hair

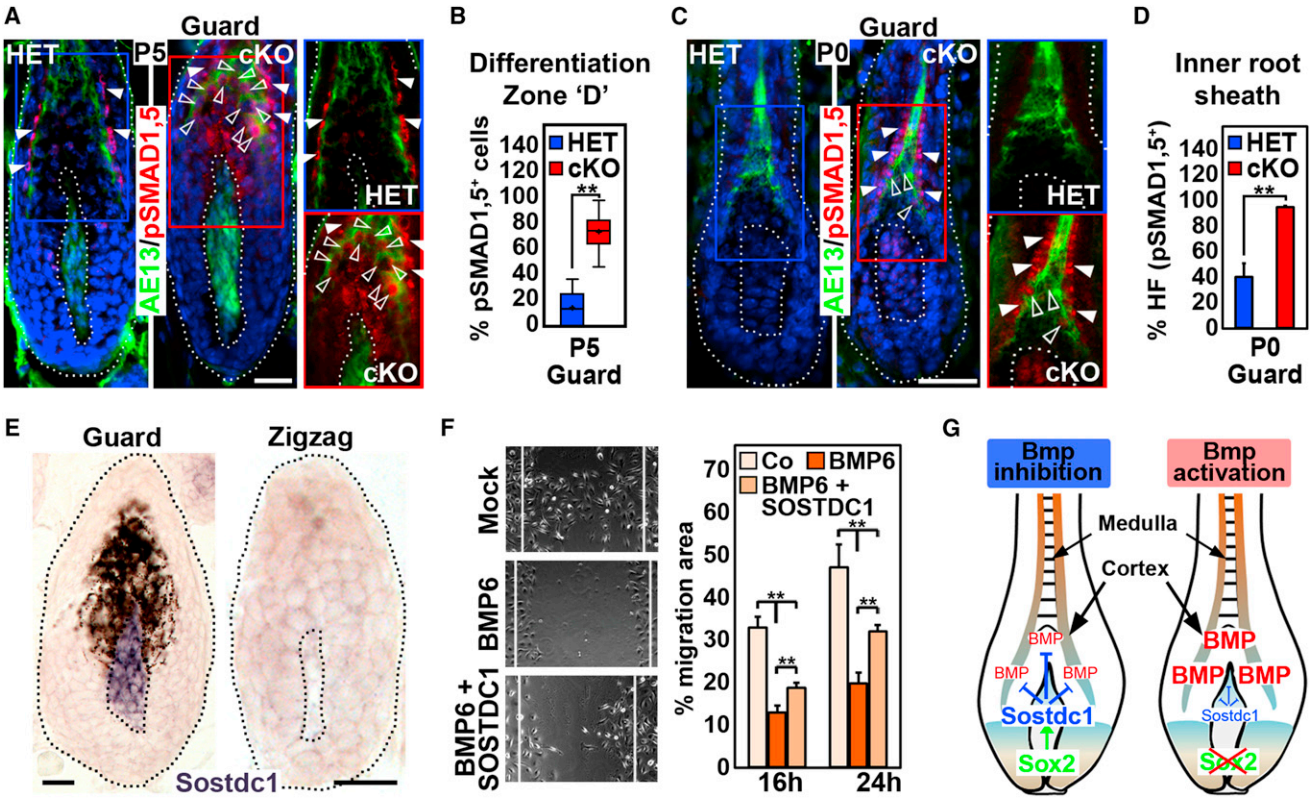


**Figure 6. Increased BMP Signaling in Differentiating Hair Shaft Lineages in *Sox2* Ablated Guard Hair Follicles**

(A) Immunofluorescence for pSMAD1,5 in P5 *Sox2*$^{GFP}$ HET and cKO guard hair follicles. AE13 highlights differentiating hair cortex (green). GFP signal in the DP is from *Sox2*$^{GFP}$. Normal BMP signaling in IRS (arrowheads). BMP signaling in hair cortex progenitors is upregulated in cKO (open arrowheads). Nuclei are counterstained with DAPI. Right: blue (HET) and red (cKO) inserts without DAPI.

(B) Quantification of pSMAD1,5-positive cells within the AE13 domain of P5 guard hair follicles.

(C) pSMAD1,5 immunofluorescence at P0. Precocious BMP signaling in IRS (arrowheads) and hair cortex (open arrowheads) in cKO follicles. BMP activity is also increased in upper DP.

(D) Quantification of hair follicles (HF) with pSMAD1,5-positive IRS/hair cortex progenitors in guard hair follicles at P0.

(E) In situ hybridization for *Sostdc1* mRNA expression in Sox2 guard and zigzag hair follicle. Dotted line marks the basement membrane.

(F) In vitro scratch migration assay. BMP6 (500 ng/ml) decreases migration of skin epithelial cells, which is alleviated by SOSTDC1 (300 ng/ml). Right: Quantification of migrated area. Data are mean ± SEM from two independent experiments. **p < 0.01.

(G) Model of fine-tuning BMP signaling in hair shaft progenitors. *Sox2* in the DP niche drives the expression of BMP inhibitor *Sostdc1*, counteracting BMPs produced by matrix cells at the base and by the DP to fine-tune BMP signaling in differentiating hair shaft progenitors. In follicles with *Sox2* null DPs, the equilibrium is unbalanced leading to increased BMP signaling and decreased migration during hair shaft differentiation.

All box-and-whisker plots: mid-line, median; mean, plus symbol; box, 25$^{th}$ and 75$^{th}$ percentiles; whiskers, 10$^{th}$ and 90$^{th}$ percentiles. N = 10 guard and zigzag hairs. Counts are from two independent experiments. **p < 0.01. All scale bars are 25 μm.

See also Figure S4.

follicles (Figure 6C, arrowheads), compared to only few cells in ~38% of HET guard hairs (Figure 6D). Few AE13-positive hair cortex (Figure 6C, open arrowheads) and DP cells were also pSMAD1,5-positive in cKO guard hair follicles. This suggested that over the course of at least 5 days during early postnatal hair growth, BMP signaling was precociously activated and increased in differentiating hair shaft cells in *Sox2* cKO follicles.

## Reduced Hair Growth Speed and Increased BMP Signaling Activity in *Sox2*-Negative Zigzag Hair Follicles

We next wondered about the level of hair shaft cell migration and BMP signaling activation in zigzag hair follicles, the *Sox2*-negative (Figure 1C) and shortest hair type (Figure 2E). First, we determined whether, as predicted, the percentage of BrdU$^{+}$ cells entering the differentiation zone "D" is similar in HET and cKO zigzag hair follicles. Unsurprisingly, the number of traced cells is not reduced in *Sox2* cKO zigzag follicles compared to HET controls, because this follicle type does not express *Sox2* (Figure S4C). Because zigzag follicles are much smaller than guard hairs and our quantification of labeled cells in zones only measures relative migration speed in comparably sized follicles, we established an absolute measurement of migration speed by determining the total distance that cells traveled from the time after pulse (2 hr, top level of the DP) to the highest location in the differentiating compartment at 24 hr (Figure S4D). With this absolute speed measurement, we determined that migration of hair shaft progenitors in HET and cKO zigzag follicles was much slower than that in normal guard hairs, and that cell

migration speed in cKO guard hairs is reduced and becomes more similar to the speed of zigzag follicles (Figure S4E). Importantly, zigzag follicles by default also express high levels of active pSMAD1,5 (Figures S4F and S4G, open arrowheads), comparable to *Sox2* cKO guard hairs (Figures 6B), linking slower migration and hair growth with increased BMP signaling activity. Interestingly, DPs in zigzag follicles also lack *Sostdc1* expression (Figure 6E), suggesting a permissive state for increased BMP activity in differentiating hair shaft lineages.

### BMP Signaling Inhibits Cell Migration, Which Can Be Attenuated by Sostdc1

Because BMP signaling has previously been shown to inhibit cell migration (Kaiser et al., 1998), we finally tested whether *Bmp6* and *Sostdc1* could directly affect migration of skin epithelial cells in vitro to help mechanistically explain slowed movement of matrix cells from the proliferating into the differentiating compartments in *Sox2* cKO follicles. In a well-established scratch migration assay, proliferation-inhibited cells migrated toward the center of the scratch within 24 hr, as expected (Figure 6F). This was significantly reduced in the presence of BMP6, but could be partially restored by addition of SOSTDC1, demonstrating that BMP signaling directly affects cell migration. It also indicates that the level of BMP signaling activity as the outcome of positive and negative regulators determines the extent of migration speed and further suggests that the level of secreted BMP signaling regulators from the DP niche, controlled by *Sox2,* fine-tunes migration of hair shaft progenitors during hair growth.

## DISCUSSION

Although robust expression of *Sox2* in DP niche cells during hair follicle formation and growth was first described years ago, the function of this transcription factor and of many other genes has been unexplored largely due to the long-standing absence of genetic tools to target the DP for gene ablation. Very recently, two Cre recombinase expressing lines were introduced to study the function of DP genes (Enshell-Seijffers et al., 2010; Lehman et al., 2009; Woo et al., 2012). *Prx1-Cre* broadly targets the dermis several days before the start of hair morphogenesis, but is limited to the limbs and focal areas in ventral skin (Logan et al., 2002) where the timing of hair development and the distribution of hair types is not well understood. *Corin*$^{Cre}$ is active specifically in DP cells throughout the backskin, where hair development is well defined, but does not fully ablate genes before postnatal day P7 (Enshell-Seijffers et al., 2010). Here, we use *Tbx18*$^{Cre}$ to target embryonic DP precursors in the backskin (Grisanti et al., 2012) to interrogate the functional role of the DP signature gene *Sox2* during hair follicle formation and growth.

With our work, we identify a striking reduction of postnatal hair shaft lengths in *Sox2* null guard and awl/auchene hair follicles. Although hair follicles and shafts did form normally, they grew out at continuously reduced rates due to delayed migration of differentiating hair shaft progenitors. Surprisingly, matrix progenitor proliferation was not affected, increased cell death did not occur and differentiation into IRS and hair shaft cell lineages was normal as well. This is an unusual finding since direct gene manipulations in the hair follicle epithelium typically result in strongly altered proliferation or differentiation phenotypes (Alonso et al., 2005; Andl et al., 2004; Ezhkova et al., 2011; Kaufman et al., 2003; Kobielak et al., 2003; Kulessa et al., 2000). It also suggests that signals from the mesenchymal DP niche under the transcriptional control of *Sox2* fine-tune the rate of epithelial hair shaft outgrowth by affecting hair shaft progenitor migration rather than regulating the global proliferation and differentiation programs.

Our comprehensive molecular analysis with microarrays and real-time PCR in freshly isolated knockout DPs revealed multiple altered genes that could directly or indirectly cause the observed hair shaft growth phenotype. Among the most strongly regulated genes were BMP pathway members that stood out because the BMP pathway has been shown previously to regulate proliferation, migration and differentiation of hair follicle and epidermal epithelial cells (Andl et al., 2004; Blessing et al., 1993; Kaiser et al., 1998; Kobielak et al., 2003; Kulessa et al., 2000). In *Sox2* null DPs, we found that the BMP ligand *Bmp6* was upregulated and expression of BMP/WNT inhibitor *Sostdc1* was strongly decreased. This suggested a potential shift toward increased BMP signaling activity in DP, surrounding matrix cells at the follicle base and/or differentiating hair shaft lineages due to loss of *Sox2* in the DP. Indeed, we found precocious and increased BMP signaling in hair shaft progenitors on their journey toward becoming terminally differentiated hair shaft and IRS. Interestingly, we did not observe increased BMP signaling in highly proliferative matrix cells at the follicle base. This suggests a gradient model where BMP regulators produced by the DP locally fine-tune BMP signaling activity at the follicle mid-level, but not at its proliferative base, to control hair shaft progenitor migration. In addition, we found increased autocrine BMP signaling in the upper DP itself, which could indirectly contribute to regulating hair growth speed through additional downstream BMP targets in the DP.

Much as proliferation within the hair follicle was unchanged, we found that increased BMP signaling activity in hair shaft progenitors did not cause any disturbance of normal hair shaft differentiation. Conversely, severe hair shaft differentiation phenotypes were observed in studies of BMP signaling inhibition by receptor ablation (Andl et al., 2004; Kobielak et al., 2003) or misexpression of the inhibitor *Noggin* (Kulessa et al., 2000), suggesting that BMP signaling is required for differentiation, but increased, precocious signaling interferes with migration rather than differentiation. In our study, reduced cell migration is the most likely explanation for slowed matrix cell transition into the differentiating compartment, which is consistent with previous reports showing that increased BMP signaling activity can cause reduced cell migration (Ahmed et al., 2011; Kaiser et al., 1998). Indeed, our tests of direct effects of BMP6 and SOSTDC1 on primary skin epithelial cell migration revealed inhibition of migration by BMP6 that could be alleviated by SOSTDC1. This supports a model (Figure 6G), in which *Sox2* in the DP niche controls the expression of BMP inhibitor SOSTDC1 and BMP6 to fine-tune epithelial BMP signaling activity for proper timing of hair shaft progenitor cell migration.

Recent global ablation of *Sostdc1* in full knockout mice did not cause reduced postnatal hair growth phenotypes (Närhi et al., 2012). Because both downregulated *Sostdc1* and upregulated *Bmp6* were observed in *Sox2* cKO DPs, the simultaneous

differential regulation of both BMP inhibitor and ligand may be essential for precisely fine-tuning levels of BMP signaling activity to affect hair growth. Increased BMP signaling in the DP of *Sox2* mutants may also cause additional downstream effects that could influence the speed of hair growth. In *Sostdc1* null embryos, hair follicle numbers and placode sizes are increased (Närhi et al., 2012). At that stage, *Sostdc1* is expressed in the epidermis at the edges of placodes and appears to act as WNT inhibitor to limit the extent of WNT signaling, without any evidence of inhibiting BMP signaling. In *Sox2* null follicles that lack *Sostdc1* during postnatal hair growth, we did not find increased or expanded nuclear β-catenin, suggesting that WNT signaling does not directly contribute to altered hair shaft progenitor migration. Increased nuclear β-catenin in the DP itself suggests increased WNT signaling in the DP, which could indirectly affect hair growth speed through WNT targets in the DP (Enshell-Seijffers et al., 2010).

Our observation that shorter *Sox2*-negative zigzag hair follicles exhibit molecular and cell migration features similar to *Sox2* cKO guard hairs reveals the physiologic significance of the connection between *Sox2* regulation of BMP ligand/inhibitor in the DP and BMP pathway activation and migration speed in hair shaft progenitors. By default, BMP signaling activity is increased and migration speed is decreased in zigzag hair follicles, much like in guard hair follicles after ablation of *Sox2*, likely contributing to slower hair growth in this hair type. However, it should be noted that these two hair follicle types were at different developmental stages in our analysis, as zigzag follicles develop several days after guard hairs. As global BMP signaling progressively increases in postnatal back skin (Andl et al., 2004), it is possible that additional *Sox2*-independent factors drive the observed BMP signaling and migration differences between guard and zigzag hair follicles. As *Sox2* cKO guard hairs grow slower but otherwise retain all other size, form, and shape features without becoming more "zigzag like," *Sox2* likely does not constitute a master transcriptional regulator of overall hair type fate, but appears to be a bona fide key regulator of hair growth speed. In summary, our findings demonstrate that *Sox2*, as a direct transcriptional regulator in the DP, controls niche signals that act on surrounding hair shaft progenitors in the mesenchymal-epithelial crosstalk that orchestrates the speed of hair follicle growth.

## EXPERIMENTAL PROCEDURES

### Mice

$Sox2^{fl/fl}$ and $Sox2^{GFP/+}$ knockin and Lef1-RFP transgenic lines were previously described (Ellis et al., 2004; Favaro et al., 2009; Rendl et al., 2005). $Tbx18^{LacZ/+}$ was previously described (Cai et al., 2008). The previously published $Tbx18^{Cre/+}$ knockin line (Cai et al., 2008) was modified to remove neomycin through genetic crossing with a *FLP* deleter line. $R26R^{LacZ}$ reporter mice (Soriano, 1999) were obtained from Jackson Laboratories (Bar Harbor, ME). For 5-bromo-2′-deoxyuridine (BrdU) pulse experiments, mice were injected intraperitoneally with 50 mg/g BrdU (Sigma-Aldrich). All animal experiments were performed in accordance with the guidelines and approval of the Institutional Animal Care and Use Committee at Mount Sinai School of Medicine.

### Histology, Immunofluorescence, and In Situ Hybridization

Histology, immunofluorescence, and in situ hybridization were carried out as described previously (Rendl et al., 2005; Grisanti et al., 2012). Details of antibodies and probes are provided in Supplemental Experimental Procedures.

### Chromatin Immunoprecipitation

Chromatin immunoprecipitation was performed according to manufacturer's instructions using the EZ-Magna ChIP kit (Millipore) and sorted DP cell extracts. Cells were fixed in 1% formaldehyde, lysed, and chromatin was sonicated to 200 base pair fragments. Chromatin was immunoprecipitated with SOX2 antibodies (Millipore) or control IgG. RT-PCR and real-time PCR were performed with the LightCycler system and DNA master SYBR Green I reagents (Roche). Relative binding was calculated with the $2^{-\Delta\Delta CT}$ method. Binding site specific primer sequences are provided in Supplemental Experiment Procedures.

### In Vitro Scratch Migration Assay

Primary early passage keratinocytes were cultured in 6-well plates until reaching confluence, starved in serum-free basal medium for 20 hr, followed by 10 μg/ml mitomycin C for 2 hr. A straight scratch was made with a pipet tip, followed by culture with 500 ng/ml BMP6 and/or 300 ng/ml SOSTDC1 (R&D Biosystems). Phase-contrast images of 10 nonoverlapping fields in triplicate scratch wounds were taken per time point and relative areas covered by migrating cells were quantified with ImageJ.

### Cell Isolation, Real-Time PCR, and Microarray Analysis

Cell isolation, real-time PCR, and microarray analysis were carried out as described previously (Rendl et al., 2005). See Supplemental Experimental Procedures for detailed methods and primer sequences.

### Statistics

A two-tailed Student's t test was used to calculate statistical significance.

## SUPPLEMENTAL INFORMATION

Supplemental Information includes four figures and Supplemental Experimental Procedures and can be found with this article online at http://dx.doi.org/10.1016/j.devcel.2012.10.013.

## ACKNOWLEDGMENTS

We thank Valerie Horsley, Hoang Nguyen, Robert Krauss, Phil Soriano, and Tudorita Tumbar for insightful discussions and valuable comments on the manuscript and Elena Ezkhova and Jisheng Zhang for support with keratinocyte cultures. We also thank the personnel of the Mount Sinai Flow Cytometry Core Facility and NYU Genomics Core for excellent cell sorting and microarray service. This work was supported by a grant to A.M. from NIH/NIGMS (R01-GM098316) and to M.R. from NIH/NIAMS (R01-AR059143).

Received: July 25, 2012
Revised: September 25, 2012
Accepted: October 16, 2012
Published online: November 12, 2012

## REFERENCES

Ahmed, M.I., Mardaryev, A.N., Lewis, C.J., Sharov, A.A., and Botchkareva, N.V. (2011). MicroRNA-21 is an important downstream component of BMP signalling in epidermal keratinocytes. J. Cell Sci. *124*, 3399–3404.

Alonso, L., Okada, H., Pasolli, H.A., Wakeham, A., You-Ten, A.I., Mak, T.W., and Fuchs, E. (2005). Sgk3 links growth factor signaling to maintenance of progenitor cells in the hair follicle. J. Cell Biol. *170*, 559–570.

Andl, T., Ahn, K., Kairo, A., Chu, E.Y., Wine-Lee, L., Reddy, S.T., Croft, N.J., Cebra-Thomas, J.A., Metzger, D., Chambon, P., et al. (2004). Epithelial Bmpr1a regulates differentiation and proliferation in postnatal hair follicles and is essential for tooth development. Development *131*, 2257–2268.

Arnold, K., Sarkar, A., Yram, M.A., Polo, J.M., Bronson, R., Sengupta, S., Seandel, M., Geijsen, N., and Hochedlinger, K. (2011). Sox2(+) adult stem

and progenitor cells are important for tissue regeneration and survival of mice. Cell Stem Cell *9*, 317–329.

Biernaskie, J., Paris, M., Morozova, O., Fagan, B.M., Marra, M., Pevny, L., and Miller, F.D. (2009). SKPs derive from hair follicle precursors and exhibit properties of adult dermal stem cells. Cell Stem Cell *5*, 610–623.

Blanpain, C., and Fuchs, E. (2009). Epidermal homeostasis: a balancing act of stem cells in the skin. Nat. Rev. Mol. Cell Biol. *10*, 207–217.

Blessing, M., Nanney, L.B., King, L.E., Jones, C.M., and Hogan, B.L. (1993). Transgenic mice as a model to study the role of TGF-beta-related molecules in hair follicles. Genes Dev. *7*, 204–215.

Boyer, L.A., Lee, T.I., Cole, M.F., Johnstone, S.E., Levine, S.S., Zucker, J.P., Guenther, M.G., Kumar, R.M., Murray, H.L., Jenner, R.G., et al. (2005). Core transcriptional regulatory circuitry in human embryonic stem cells. Cell *122*, 947–956.

Cai, C.L., Martin, J.C., Sun, Y., Cui, L., Wang, L., Ouyang, K., Yang, L., Bu, L., Liang, X., Zhang, X., et al. (2008). A myocardial lineage derives from Tbx18 epicardial cells. Nature *454*, 104–108.

DasGupta, R., and Fuchs, E. (1999). Multiple roles for activated LEF/TCF transcription complexes during hair follicle development and differentiation. Development *126*, 4557–4568.

Driskell, R.R., Giangreco, A., Jensen, K.B., Mulder, K.W., and Watt, F.M. (2009). Sox2-positive dermal papilla cells specify hair follicle type in mammalian epidermis. Development *136*, 2815–2823.

Driskell, R.R., Clavel, C., Rendl, M., and Watt, F.M. (2011). Hair follicle dermal papilla cells at a glance. J. Cell Sci. *124*, 1179–1182.

Ellis, P., Fagan, B.M., Magness, S.T., Hutton, S., Taranova, O., Hayashi, S., McMahon, A., Rao, M., and Pevny, L. (2004). SOX2, a persistent marker for multipotential neural stem cells derived from embryonic stem cells, the embryo or the adult. Dev. Neurosci. *26*, 148–165.

Enshell-Seijffers, D., Lindon, C., Kashiwagi, M., and Morgan, B.A. (2010). beta-catenin activity in the dermal papilla regulates morphogenesis and regeneration of hair. Dev. Cell *18*, 633–642.

Ezhkova, E., Lien, W.H., Stokes, N., Pasolli, H.A., Silva, J.M., and Fuchs, E. (2011). EZH1 and EZH2 cogovern histone H3K27 trimethylation and are essential for hair follicle homeostasis and wound repair. Genes Dev. *25*, 485–498.

Fang, X., Yoon, J.G., Li, L., Yu, W., Shao, J., Hua, D., Zheng, S., Hood, L., Goodlett, D.R., Foltz, G., and Lin, B. (2011). The SOX2 response program in glioblastoma multiforme: an integrated ChIP-seq, expression microarray, and microRNA analysis. BMC Genomics *12*, 11.

Favaro, R., Valotta, M., Ferri, A.L., Latorre, E., Mariani, J., Giachino, C., Lancini, C., Tosetti, V., Ottolenghi, S., Taylor, V., and Nicolis, S.K. (2009). Hippocampal development and neural stem cell maintenance require Sox2-dependent regulation of Shh. Nat. Neurosci. *12*, 1248–1256.

Ferri, A.L., Cavallaro, M., Braida, D., Di Cristofano, A., Canta, A., Vezzani, A., Ottolenghi, S., Pandolfi, P.P., Sala, M., DeBiasi, S., and Nicolis, S.K. (2004). Sox2 deficiency causes neurodegeneration and impaired neurogenesis in the adult mouse brain. Development *131*, 3805–3819.

Greco, V., Chen, T., Rendl, M., Schober, M., Pasolli, H.A., Stokes, N., Dela Cruz-Racelis, J., and Fuchs, E. (2009). A two-step mechanism for stem cell activation during hair regeneration. Cell Stem Cell *4*, 155–169.

Grisanti, L., Clavel, C., Cai, X., Rezza, A., Tsai, S.Y., Sennett, R., Mumau, M., Cai, C.L., and Rendl, M. (2012). Tbx18 targets dermal condensates for labeling, isolation, and gene ablation during embryonic hair follicle formation. J Invest Dermatol., in press. Published online September 20, 2012. http://dx.doi.org/10.1038/jid.2012.329.

Hardy, M.H. (1992). The secret life of the hair follicle. Trends Genet. *8*, 55–61.

Hsu, Y.C., and Fuchs, E. (2012). A family business: stem cell progeny join the niche to regulate homeostasis. Nat. Rev. Mol. Cell Biol. *13*, 103–114.

Kaiser, S., Schirmacher, P., Philipp, A., Protschka, M., Moll, I., Nicol, K., and Blessing, M. (1998). Induction of bone morphogenetic protein-6 in skin wounds. Delayed reepitheliazation and scar formation in BMP-6 overexpressing transgenic mice. J. Invest. Dermatol. *111*, 1145–1152.

Kaufman, C.K., Zhou, P., Pasolli, H.A., Rendl, M., Bolotin, D., Lim, K.C., Dai, X., Alegre, M.L., and Fuchs, E. (2003). GATA-3: an unexpected regulator of cell lineage determination in skin. Genes Dev. *17*, 2108–2122.

Kishimoto, J., Burgeson, R.E., and Morgan, B.A. (2000). Wnt signaling maintains the hair-inducing activity of the dermal papilla. Genes Dev. *14*, 1181–1185.

Kobielak, K., Pasolli, H.A., Alonso, L., Polak, L., and Fuchs, E. (2003). Defining BMP functions in the hair follicle by conditional ablation of BMP receptor IA. J. Cell Biol. *163*, 609–623.

Kraus, F., Haenig, B., and Kispert, A. (2001). Cloning and expression analysis of the mouse T-box gene Tbx18. Mech. Dev. *100*, 83–86.

Kulessa, H., Turk, G., and Hogan, B.L.M. (2000). Inhibition of Bmp signaling affects growth and differentiation in the anagen hair follicle. EMBO J. *19*, 6664–6674.

Lee, J., Basak, J.M., Demehri, S., and Kopan, R. (2007). Bi-compartmental communication contributes to the opposite proliferative behavior of Notch1-deficient hair follicle and epidermal keratinocytes. Development *134*, 2795–2806.

Lee, J., and Tumbar, T. (2012). Hairy tale of signaling in hair follicle development and cycling. Semin. Cell Dev. Biol, in press. Published online August 21, 2012. http://dx.doi.org/10.1016/j.semcdb.2012.08.003.

Lehman, J.M., Laag, E., Michaud, E.J., and Yoder, B.K. (2009). An essential role for dermal primary cilia in hair follicle morphogenesis. J. Invest. Dermatol. *129*, 438–448.

Logan, M., Martin, J.F., Nagy, A., Lobe, C., Olson, E.N., and Tabin, C.J. (2002). Expression of Cre Recombinase in the developing mouse limb bud driven by a Prxl enhancer. Genesis *33*, 77–80.

Massagué, J., Seoane, J., and Wotton, D. (2005). Smad transcription factors. Genes Dev. *19*, 2783–2810.

Merrill, B.J., Gat, U., DasGupta, R., and Fuchs, E. (2001). Tcf3 and Lef1 regulate lineage differentiation of multipotent stem cells in skin. Genes Dev. *15*, 1688–1705.

Millar, S.E. (2002). Molecular mechanisms regulating hair follicle development. J. Invest. Dermatol. *118*, 216–225.

Moore, K.A., and Lemischka, I.R. (2006). Stem cells and their niches. Science *311*, 1880–1885.

Müller-Röver, S., Handjiski, B., van der Veen, C., Eichmüller, S., Foitzik, K., McKay, I.A., Stenn, K.S., and Paus, R. (2001). A comprehensive guide for the accurate classification of murine hair follicles in distinct hair cycle stages. J. Invest. Dermatol. *117*, 3–15.

Närhi, K., Tummers, M., Ahtiainen, L., Itoh, N., Thesleff, I., and Mikkola, M.L. (2012). Sostdc1 defines the size and number of skin appendage placodes. Dev. Biol. *364*, 149–161.

Nowak, J.A., Polak, L., Pasolli, H.A., and Fuchs, E. (2008). Hair follicle stem cells are specified and function in early skin morphogenesis. Cell Stem Cell *3*, 33–43.

Pevny, L.H., and Nicolis, S.K. (2010). Sox2 roles in neural stem cells. Int. J. Biochem. Cell Biol. *42*, 421–424.

Rendl, M., Lewis, L., and Fuchs, E. (2005). Molecular dissection of mesenchymal-epithelial interactions in the hair follicle. PLoS Biol. *3*, e331.

Rendl, M., Polak, L., and Fuchs, E. (2008). BMP signaling in dermal papilla cells is required for their hair follicle-inductive properties. Genes Dev. *22*, 543–557.

Richardson, G.D., Fantauzzo, K.A., Bazzi, H., Määttä, A., and Jahoda, C.A. (2009). Dynamic expression of Syndecan-1 during hair follicle morphogenesis. Gene Expr. Patterns *9*, 454–460.

Schlake, T. (2007). Determination of hair structure and shape. Semin. Cell Dev. Biol. *18*, 267–273.

Schneider, M.R., Schmidt-Ullrich, R., and Paus, R. (2009). The hair follicle as a dynamic miniorgan. Curr. Biol. *19*, R132–R142.

Sennett, R., and Rendl, M. (2012). Mesenchymal-epithelial interactions during hair follicle morphogenesis and cycling. Semin. Cell Dev. Biol, in press. Published online August 31, 2012. http://dx.doi.org/10.1016/j.semcdb.2012.08.011.

Soriano, P. (1999). Generalized lacZ expression with the ROSA26 Cre reporter strain. Nat. Genet. *21*, 70–71.

Takahashi, K., and Yamanaka, S. (2006). Induction of pluripotent stem cells from mouse embryonic and adult fibroblast cultures by defined factors. Cell *126*, 663–676.

Taranova, O.V., Magness, S.T., Fagan, B.M., Wu, Y., Surzenko, N., Hutton, S.R., and Pevny, L.H. (2006). SOX2 is a dose-dependent regulator of retinal neural progenitor competence. Genes Dev. *20*, 1187–1202.

Tsai, S.Y., Clavel, C., Kim, S., Ang, Y.S., Grisanti, L., Lee, D.F., Kelley, K., and Rendl, M. (2010). Oct4 and klf4 reprogram dermal papilla cells into induced pluripotent stem cells. Stem Cells *28*, 221–228.

Vanscott, E.J., Ekel, T.M., and Auerbach, R. (1963). Determinants of Rate and Kinetics of Cell Division in Scalp Hair. J. Invest. Dermatol. *41*, 269–273.

Walker, M.R., Patel, K.K., and Stappenbeck, T.S. (2009). The stem cell niche. J. Pathol. *217*, 169–180.

Woo, W.M., Zhen, H.H., and Oro, A.E. (2012). Shh maintains dermal papilla identity and hair morphogenesis via a Noggin-Shh regulatory loop. Genes Dev. *26*, 1235–1246.

Yang, C.C., and Cotsarelis, G. (2010). Review of hair follicle dermal cells. J. Dermatol. Sci. *57*, 2–11.